A DIELECTROPHORESIS FORCE DRIVEN TUNABLE CAPACITOR

by

Wenbo Li

Bachelor of Science, China University of Petroleum, 2016

Submitted to the Graduate Faculty of

Swanson School of Engineering in partial fulfillment

of the requirements for the degree of

Master of Science

University of Pittsburgh

2018

UNIVERSITY OF PITTSBURGH

SWANSON SCHOOL OF ENGINEERING

This thesis was presented

by

Wenbo Li

It was defended on

July 3, 2018

and approved by

Cho Sung Kwon, Ph.D., Professor,

Department of Mechanical Engineering and Materials Science

Chun Young Jae, Ph.D.,

Department of Industrial Engineering

Lee Sangyoep, Ph.D.,

Department of Mechanical Engineering and Materials Science

Thesis Advisor: Cho Sung Kwon, Ph.D., Professor, Department of Mechanical Engineering and Materials Science

A DIELECTROPHORESIS FORCE DRIVEN TUNABLE CAPACITOR

Wenbo Li, M.S.

University of Pittsburgh, 2018

In this article, spreading dielectric fluid using two parallel electrodes is studied under increasing voltage. As fluid is drawn out by an increasing dielectrophoresis (DEP) force, phenomenon of a sudden liquid-spreading was discovered. Gibbs free energy method was used to study this phenomenon, a reasonable explanation was given on this phenomenon.

Then, electric shape influence on the sudden liquid spreading voltage was studied, electrode width and gap was utilized to design electrode shapes. Several electrode shapes have been fabricated and tested. Designed electrodes were able to drive fluid out into the electrode and back into the reservoir again. An Appropriate electrode shape has been utilized so that the fluid length to voltage relationship was nicely linear. Driving fluid in and out of the reservoir was easily controllable.

Using this new driving method, a new concept tunable capacitor is fabricated, voltage is used to drive fluid in and out of the electrode to tune capacitance. Because of the large permittivity difference, tuning range of 0.2-1.4 pF and 0.7-3.0 pF were tested and, maximum quality factor of 600 and 250 were tested.

TABLE OF CONTENTS

LIST OF FIGURES

ACKNOWLEDGEMENT

Upon my finishing thesis defense, I have a lot of gratitude to make.

First of all, I would like to show my deepest gratitude to my advisor, Dr. Cho Sung kwon, who is really patient, thought provoking, and have provided me an environment where I can work hard and figure out what it is about to do research work. The help he gave was tremendous. I would also like to pay my sincere thanks to my committee members, Dr. and Dr. for their support and encouragement for my thesis.

Secondly, I would like to thank all my peers in the laboratory, Hongyao, Dr. Hur, Fangwei and Tony. And the advices they gave were incredible. They have given me all the encouragement I needed to finish this thesis. They have taught me every step along the way, about how to do research, and every procedure in the clean room and the lab. Their generosity is deeply appreciated. Without their help I could not have gone this far.

Last but not least, my thanks also go to my parents, without their support I wouldn't even have an opportunity to come and participated in this program. Their help wasn't only financial, they have continuously been encouraging me to go further when I was growing up. Also, I would like to show my thanks to my dear girlfriend, Xueqi Li, who has encouraged me along the way. I can't imagine doing this without her.

I also place on record, my sense of gratitude to one and all, who directly or indirectly, have lend their hand in this venture.

1.0 INTRODUCTION

1.1 CAPACITOR BACKGROUND

Tuning ratio and quality factor are main factors to determine the quality of a tunable capacitors. Tuning ratio shows how the capacitance changes, while quality factor shows how much energy is lost. Capacitors structured with high quality factor and tuning ratio capacitors have been fabricated and studied for some time. Largest tuning range comes from the tuning of moving fluids in between both electrodes. Typical tunable capacitors usually have the common structure of a comb [1] [2] [3] [4] [5]. In this way, space is optimized to produce a large capacitance. An actuator is usually used for tuning the capacitance, electric force, magnetic force, thermal expansion and other properties, which are used as actuators to generate displacement in comb structures.

1.1.1 MEMS Capacitors

Jun-Bo-Yoon [5] fabricated a capacitor with the classic comb structure. Dielectric material is placed in between the top and bottom plate and connected to a spring structure, then an electrostatic force is used to move dielectric material in and out of the plate. In this way, a maximum

capacitance change of 40% was determined with a quality factor of 290 at 1 GHz frequency. In the same year, a single plate capacitor [6] is brought up by the same actuation method, a 500×500 micron structure was built to achieve a tuning range of 69%, in this research, the pull in effect was the main cause of a small tuning range, once the voltage reaches a threshold value, electrostatic force between the top and bottom plate becomes so strong that they are attracted together. Then, in Robert L's article [4], a tunable capacitor designed for 225-400MHz can have a quality factor of over 100 and a tuning ratio of about 8.4 to 1 with capacitance range of 1.4-11.9pF [4]. Utilizing a CMOS micromachining process, a 352.4% tuning ratio capacitor [2] was fabricated, maximum q factor can be over 50 at 1.5GHz. Then, tunable capacitor with an electrically floating plate was introduced, instead of two plates, they used three plates to produce a capacitor. A thermal actuator was used to reach a 631% tuning range with a q factor of 24.4 was measured at 1 GHz.

1.1.2 High permittivity liquid in use of tunable capacitors

In order to achieve larger tuning range and better performance, the idea of dielectric liquids as material between capacitor electrodes has been adopted. In this way, tuning ratio not only comes from the dielectric constant difference but also from the fluidic displacements. In this way, a much bigger capacitance range was reached. At first, a capacitor was immersed in dielectric fluid, and tuning range increased by the ratio of permittivity [7]. Then, water and air were used to pass through the space in between the two plates to give a larger tuning ratio [8]. Due to large permittivity difference of water and air, a maximum tuning ratio of 6700% was seen at low frequency, a quality factor of around 16 was detected at 2.5GHz.

Furthermore, another tunable capacitor was designed and fabricated to reach a tuning ratio of 3460% and quality factor of 5.3 to 69 with a more specific design [9] [10]. A channel is built

with SU-8 photoresist and capacitor electrodes are embedded in the channel. Therefore, when the channel is filled with dielectric fluid, electrode is covered by dielectric fluid, in this way, permittivity of material between electrodes is changed, then capacitance changes.

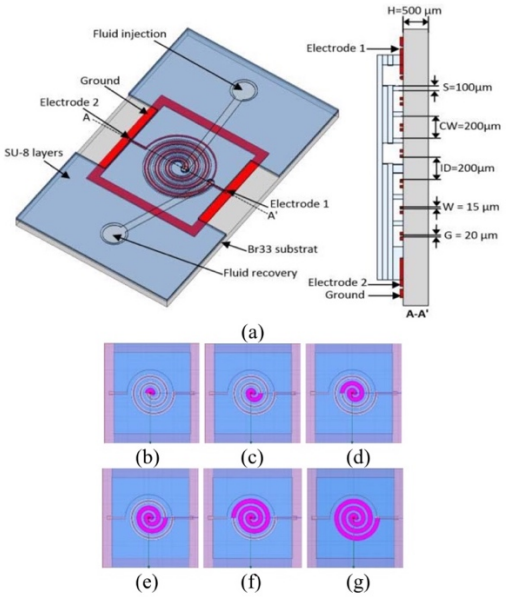

Figure 1. Capacitor structure

However, this way of manipulating liquids requires tubing, pumping and valves, with channel size this small, clogging problem can easily occur during operation. To solve this problem, dielectrophoresis (DEP) is considered in this article to move fluids around and form a tunable capacitor.

1.2 DIELECTROPHORESIS DRIVING

It is common sense that after rubbing a comb on hair, small pieces of objects, such as paper pieces, can be attracted due to electric force. This phenomenon was first named ‘dielectrophoresis’ by Phol [11], who described a motion that suspensoid particle can experience under an inhomogeneous electric field. Larger permittivity material will be moved to stronger electric field while lower permittivity materials to weaker electric field.

This phenomenon was used in fluid field and formed the dielectrophoresis force we know today. At first, nano-droplet actuation and formation was demonstrated [12] [13] [14]. Two parallel electrodes were fabricated, and the liquid was drawn out by this electrode in a rivulet shape. When voltage is turned off, droplets form along the electrode length, and the volume of the droplet is influenced by the width of electrode. In order to control the shape and number of droplets, circular shape nodes were fabricated so that when voltage is turned off, nano-droplet is formed around the circular area. In this way, fluid is distributed from the reservoir to droplets along the electrode. It is also shown that with two inclined electrodes, electric field is non-uniform, high permittivity material (water) is drawn to the larger permittivity area while low permittivity material (air) is drawn to smaller permittivity area. So, droplets are drawn to one side while bubbles are drawn the other way. By using DI water, he also distinguished the difference between electro-wetting and dielectrophoresis [15] [16].

DEP force has also been utilized to move around small particles. DNA and RNA molecules have been held by a DEP tweezer, and different size particles have been separated by DEP force. Several different electrodes have been designed, and electric fields have been drawn out [17] [18].

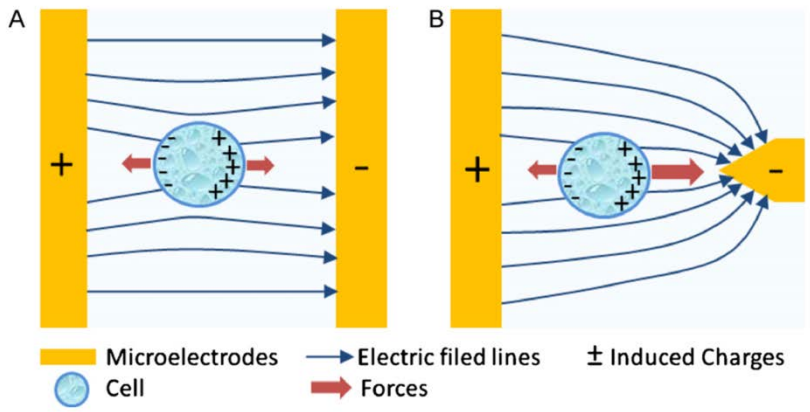

Figure 2. Inhomogeneous electric field exert force

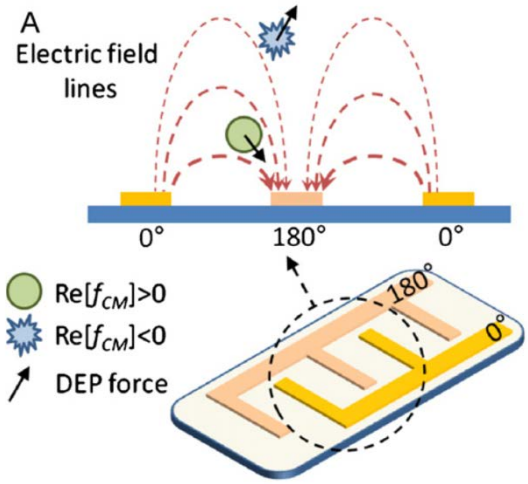

Figure 3. Fringing electric field

In Figure3, it is easy to see that strongest electric field occurs at the edge of the electrode, so high permittivity particles or fluids further from the panel are drawn to this area.

Due to this effect, Jones developed a way to drive liquid into rivulets using dielectrophoresis (DEP) force. The classic configuration is two parallel electrodes. Once actuated,

dielectric water can be spread through the panels. Fluid will be drawn to bigger permittivity area: onto the electrode and along the electrode. Similar interdigitated same widths and gaps electrode [19] [20] was first brought up to form a voltage programmable liquid optical interface. Electrodes are placed same distance from each other, when actuated, dielectric fluid is drawn towards the panel and spread into a very thin layer. The contact angle can reach almost as low as zero degree. Therefore this phenomenon is named super-spreading. The electric field of this structure [21] is an electric fringing field where its magnitude is decaying exponentially along the height direction. The difference of electric field intensity explains the spreading of dielectric fluid.

Utilizing this configuration, an interlocking continuous electrode pad was fabricated. The liquid was created, transported, merged and split [22] using only the on and off of different panels. A different configuration of DEP force is demonstrated in two plates. Once the two plates are actuated, it can move around liquids as well [23]. DEP force and electro-wetting force are both used to manipulate different materials. Silicon oil and water were driven separately, and their droplets were merged and separated [24] [25]. Bubbles were moved to the desired positions [26], and they were then merged and separated. Since a long electrode could form a long rivulet, an optical fiber was made from this configuration [27]. Light was successfully conducted using this liquid fiber.

In this article, long electrode was fabricated and formed into certain shape. Changing electrode shape was used to drive fluid to any length.

2.0 EXPERIMENTAL

Experiments are realized using in-plane electrodes, as shown in Figure 4, a capacitor consists of a reservoir, two capacitor electrodes and two driving electrodes. High permittivity fluid is stored in the reservoir. When larger capacitance is required, driving electrode is actuated to drive high permittivity fluid onto the capacitor electrode which would tune the capacitor bigger. Reservoir electrodes and capacitor electrodes are 50 μ m wide and 50 μ m apart. Driving electrodes shape might vary due to different driving ability, but they are all 50 μ m away from the capacitance electrode.

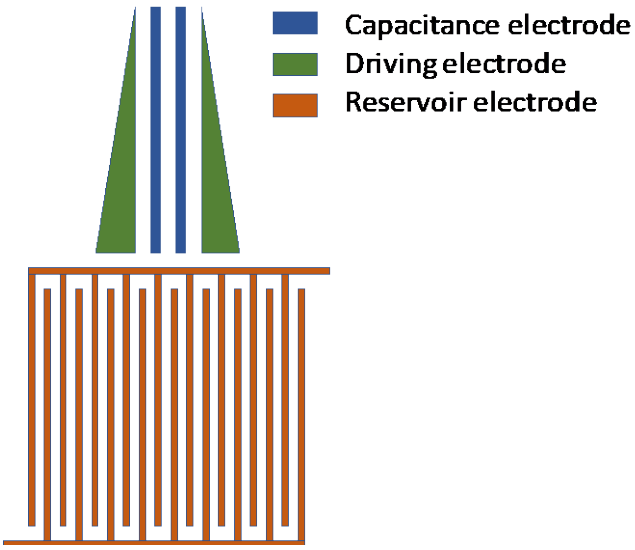

Figure 4. Capacitance structure

The whole device is made of gold and chromium: 10nm Cr and 80nm Au was deposited using e-beam evaporation onto Soda lime glass wafer. Photoresist (AZP4210) was spin coated to form uniform thickness. Then standard photolithography process was performed to transfer pattern from mask to photoresist. Wet etching was used to transfer photoresist pattern onto the metal electrode. To get an effective dielectric layer, a 3μm Parylene layer was deposited using a chemical vapor deposition (CVD) system (PDS 2010 Specialty Coating System). To achieve higher initial contact angle, a layer of Teflon-AF (DuPont-USA) was dip coated and dried (55℃, 10 min) onto the surface. Before this, Teflon-AF solution was diluted with Perfluoro-compound FC- 40 (Sigma-Aldrich, USA) solvent to 1% volume concentration.

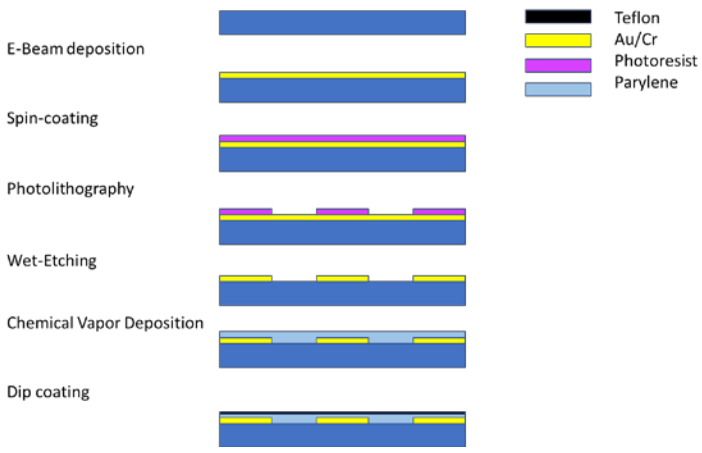

Figure 5. Process flow

Propylene carbonate (Sigma-Aldrich, USA) is used as high permittivity fluid throughout this research. It is a common non-toxic liquid with low volatility and viscosity. Its surface tension

is 42 $mN.m^{-1}$ and its relative permittivity is 65, which can both enhance the L-DEP (liquid-dielectrophoresis) force and increase the value of capacitance.

20kHz AC (alternating current) is supplied in this research. Two function generators (33220A, Agilent) are used to generate signals which is magnified by an amplifier (PZD700, trek, two channel). Then the signal is transmitted to the circuit, one to driving electrode and the other to reservoir. 280V 20kHz AC voltage is held still for reservoir while a changing magnitude 20kHz AC voltage is transmitted to the driving electrode. Voltage is read from a fluke (83-III) meter. All voltage in this research is a root mean square (V_{rms}) of the voltage value.

Real time videos are recorded using a charge-coupled device (CCD) camera (CV S3200, JAI) paired with a microscope. Fluid length is measured in videos proportionally.

In order to measure small capacitance in pF scale, the capacitor is put into a parallel circuit with a commercialized inductor. Impedance of the whole circuit is swept with an impedance analyzer (Trewmac system, TE3000). In order to reduce parasitic capacitance from connecting wires and metal electrodes, same circuit without device is used as a reference, measured reference capacitance is reduced from original data to be more accurate.

3.0 PARALLEL ELECTRODE DRVING

In the classic configuration of two electrode driving liquid, an adequate voltage is required to drive fluid out from reservoir. However, if the voltage is not enough, reservoir droplet would still change its shape. In order to control fluid length with voltage, voltage-length relationship should firstly be observed.

3.1 PARALLEL ELECTRODE DRIVING

To test relationship between voltage and fluid length, parallel electrode was used under increasing voltage. A droplet is placed in middle of the electrode, so when actuated, the droplet will be spread to both sides of the electrode, figures in this research only shows one side because the two sides are symmetric to each other. At first, droplet is elongated to an oval shape, as voltage continues to increase, a rivulet emerges from the droplet. When voltage reaches a point, a sudden much fiercer elongation of fluid is observed.

The spreading process can be divided into two states: the state in which droplet shape is changing and the state in which rivulet is stretching. The forces related are the surface tension force and the DEP force. DEP force attracts liquid out from the droplet: as the voltage increases,

DEP force increases. Surface tension force tries to retract liquid from electrodes and form a sphere shape of droplet.

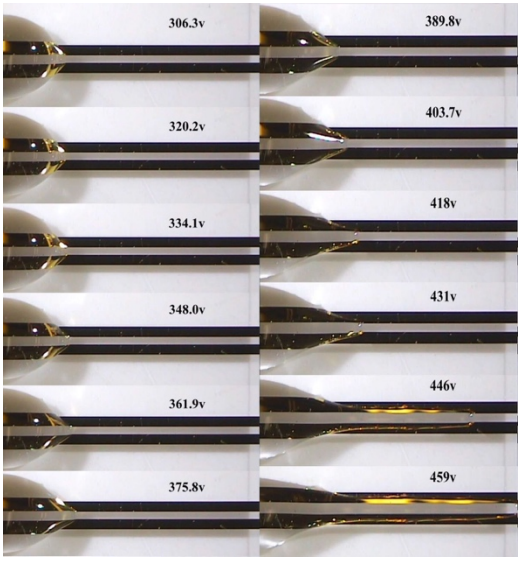

Figure 6. Sudden movement of a parallel driving electrode

The sudden burst of fluid is perceived as a domino effect. The DEP force is pulling liquid from the electrode while surface tension at the tip of the liquid is retracting liquid back. Because the electrode is parallel, the formed rivulet is of the same shape along the way, so the surface tension force is always the same once the rivulet is fully developed and its shape doesn't change anymore. Therefore, when increasing electric energy reaches a point, DEP force gets larger than surface tension, so the fluid will be spread over and over again along the electrode. However, as rivulet gets longer, the reservoir droplet is gradually getting smaller, so it should not spread infinite time.

As shown below in Figure 7, increasing voltage linearly may cause the fluid length to elongate exponentially. This makes it difficult to control fluid length using just voltage. A linear liquid length to voltage relationship is expected to give a better control.

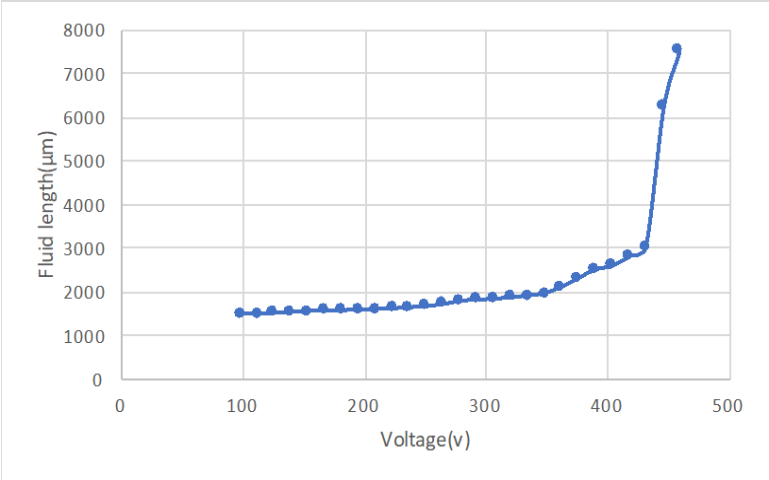

Figure 7. Fluid length-Voltage relationship

This kind of driving can also be unstable because retrieving fluid may leave behind droplet beads as shown in Figure 8. With this electrode, driving fluid out from reservoir using voltage is not a good idea.

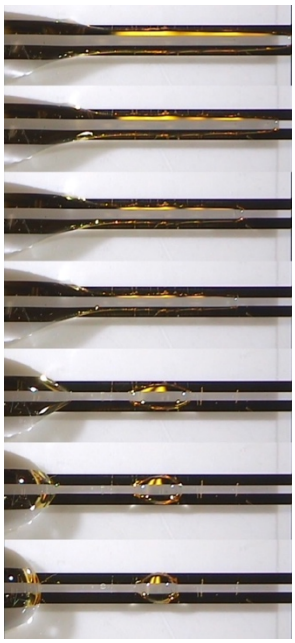

Figure 8. Droplet forming under decreasing voltage

Better electrode has to be developed so that driving fluid with voltage is better controlled.

3.2 WIDTH AND GAP INFLUENCE

From last section, it is easy to infer that a shape of electrode would have a corresponding shape of rivulet from reservoir, which would result in the corresponding amount of surface tension force. So as to compromise this surface tension energy, corresponding voltage should be applied to spread fluid. Consequently, a unique shape of electrode should have a unique actuating voltage. In order to test electrode shape influence on required voltage, electrode shape (width and gap) influence is studied in this section. The same parallel electrode experiments were conducted on

electrodes with varying width and gap, and the voltage at which fluid length starts to change suddenly is recorded and plotted below in Figure 9 and Figure 10:

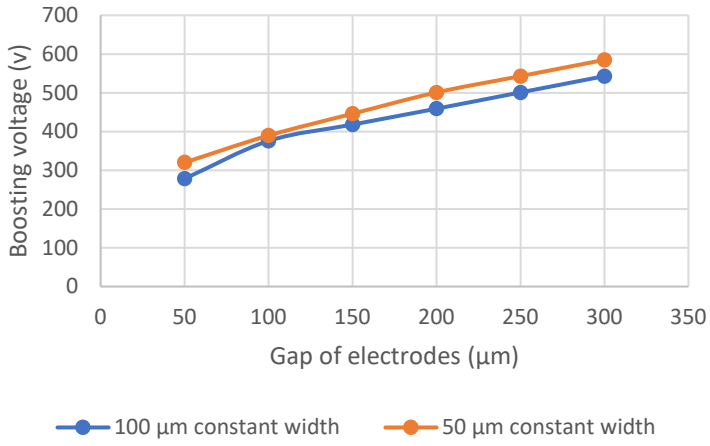

Figure 9. 50/100 μm width V_b gap relationship

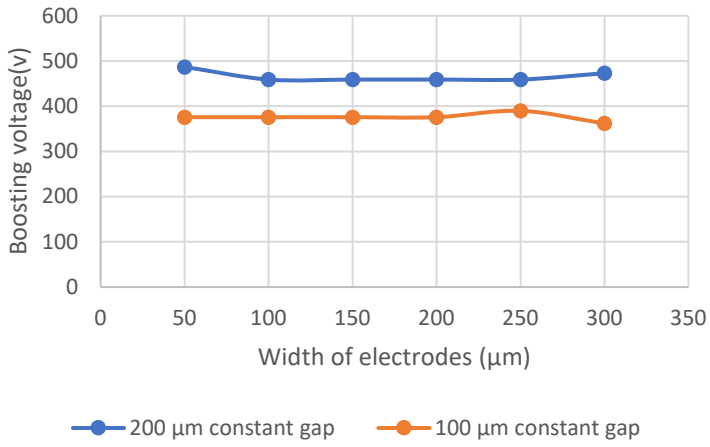

Figure 10. 100/200 μm gap V_b width relationship

It was seen in the film that the rivulet is of the same width with the electrode, so if the electrode is larger, a larger volume would be driven out. Figure 9 and Figure 10 show the relationship between this threshold voltage and electrode width and gap. It is obvious to say that as far as this experiment reaches, electrode gap has a larger influence than electrode width. This is obvious because we can see in figure 3 that the electric field is concentrated at the gap area, and gap value would influence the electric field largely. The width change wouldn't have a big impact on the electric field. However, a larger elelctrode width can also have an impact on driving by its ability to drive more fluid at one time.

3.3 THEORETICAL ANALYSIS

There are two horizontal forces affecting the elongation and retraction of droplet: DEP force and surface tension force. When droplet is spreading, two states occur: reshaping of droplet and the spreading of rivulet. Factors influencing DEP force include: dielectric layer thickness, permittivity of fluid, contact angle, electrode shape. Factors influencing surface tension are: surface tension of the system and the droplet size. In order to determine the electrode shape influence, other factors are held fixed. The wafer is fabricated with the same method, so factors such as dielectric layer thickness, permittivity, contact angle, surface tension, and droplet size are all the same among different experiments.

In order to analyze surface tension of the whole system, Gibbs free energy method was utilized. Gibbs free energy of the whole system can be expressed as:

$$\mathrm{G} = \gamma_{sl} * A_{sl} + \gamma_{sg} * A_{sg} + \gamma_{lg} * A_{lg} \quad (1)$$

When fluid spreads along the electrode, both liquid-solid and liquid-gas interface is enlarging while solid-gas interface is shrinking. Therefore, the differential of Gibbs free energy change is listed below:

$$\mathrm{dG} = \gamma_{sl} * dA_{sl} - \gamma_{sg} * dA_{sg} + \gamma_{lg} * dA_{lg} \quad (2)$$

Take an infinitesimal length of spreading liquid dl along the electrode as shown below in Figure 11.

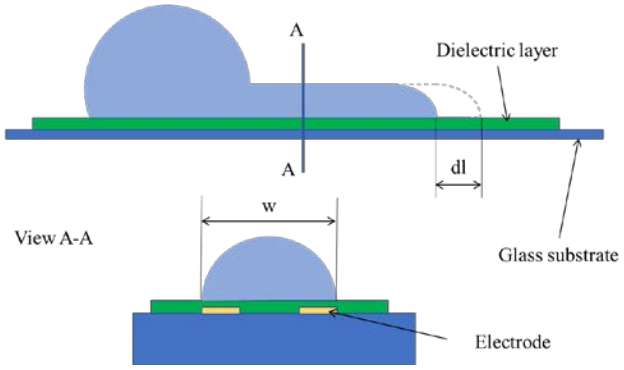

Figure 11. Electrode shape

The problem can be simplified as a sphere droplet resting on electrode. When the voltage increases, a half cylinder rivulet is driven out of the sphere droplet and the front of the rivulet is a half sphere shape.

As fluid rivulet is thin compared to droplet, and the *dl* length is infinitesimal, a small change in length of fluid rivulet wouldn't matter much to the droplet, so the droplet surface change is neglected in this consideration. So as the fluid elongates a length of dl, the solid liquid interface is

enlarged, and its shape is a square. The solid vapor interface shrunk by the same area. And the liquid vapor interface increases by a surface of a half cylinder. By using these approximations and dimensions in the problem, $dA_{sl}, dA_{sg}, dA_{lg}$ can be described as:

$$dA_{sl} = dl * w \tag{3}$$

$$dA_{sg} = dl * w \tag{4}$$

$$dA_{lg} = \frac{\pi * w}{2} * dl \tag{5}$$

Take into equation (2):

$$\mathrm{dG} = \gamma_{sl} * dl * w - \gamma_{sg} * dl * w + \gamma_{lg} * dl * \frac{\pi * w}{2} \tag{6}$$

Then the l-direction forces can be expressed as derivative of Gibbs energy with respect to l:

$$F_l = \frac{\mathrm{dG}}{\mathrm{dl}} = \left(\gamma_{sl} - \gamma_{sg}\right) * w + \gamma_{lg} * \frac{\pi * w}{2} \tag{7}$$

Since the contact angle of propylene carbonate on Teflon is 89 degrees:

$$\gamma_{sl} \cong \gamma_{sG} \tag{8}$$

So

$$F_l = \gamma_{lg} * \frac{\pi * w}{2} \tag{9}$$

From this equation, magnitude of surface tension force is illustrated as only the function of liquid width. Therefore, when the fluid is already drawn out, surface tension will not change since liquid width does not change. As the voltage is still growing, the DEP force will finally overwhelm the surface tension, which will cause the liquid length to grow exponentially.

In the state where the DEP force has not overwhelmed the surface tension yet, the two forces are in equilibrium. In this case, total Gibbs free energy can be expressed as:

$$\mathrm{G} = \gamma_{sl} * A_{sl} + \gamma_{sg} * A_{sg} + \gamma_{lg} * A_{lg} + w_e * A_{sl} \tag{10}$$

Where w_e is the electrostatic force per unit area caused by dielectrophoresis. Electric field attenuates exponentially along the height scale. By integrating the electric field over the volume of liquid, the electrostatic energy can be expressed as:

$$w_e = -\frac{\varepsilon_0 \varepsilon_l {V_0}^2}{2\delta}\left[e^{-\frac{4h}{\delta}} - 1\right] \tag{11}$$

Where $\varepsilon_0\varepsilon_l$ is permittivity of liquid. When liquid is in atmosphere, relative permittivity is $\varepsilon_0(\varepsilon_l - 1)$. $V_0$is voltage applied, δ is electric field penetration depth, and h is the liquid layer thickness. Liquid layer is much thicker than penetration depth, the above equation can be expressed as:

$$w_e = \frac{\varepsilon_0(\varepsilon_l - 1){V_0}^2}{2\delta} \tag{12}$$

In the state where liquid is first starting to expand, liquid is in a shape as illustrated in Figure 12:

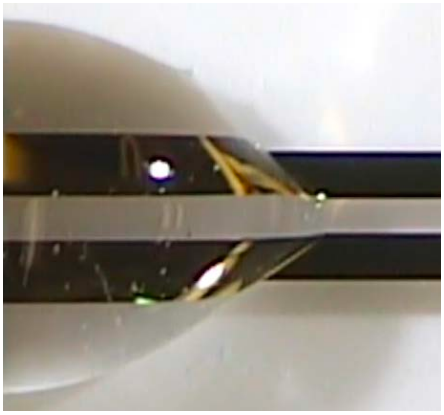

Figure 12. Fluid shape before overwhelming

Rivulet in this figure is driven by the inner electrode edge where electric field is the strongest, therefore, fluid is driven into a trapezoidal shape. In order to simplify the problem, an isosceles θ top angle triangular shaped surface and cone shaped rivulet is assumed below:

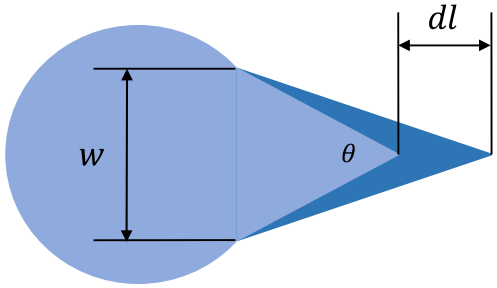

Figure 13. Fluid shape model before overwhelming

Assuming fluid stretches a distance of dl, surface change $dA_{sl}, dA_{sg}, dA_{lg}$ can be expressed as:

$$dA_{sl} = \frac{w * (l + dl)}{2} - \frac{w * l}{2} = dl * \frac{w}{2} \tag{13}$$

$$dA_{sg} = dA_{sl} = dl * \frac{w}{2} \tag{14}$$

$$dA_{lg} = \frac{1}{2} * \pi * \frac{w}{2} * dl * \cos(\frac{\theta}{2}) \tag{15}$$

Take equation (8) (12) (13) (14) (15) into equation (10),

$$\mathrm{dG} = \gamma_{lg} * \frac{1}{2} * \pi * \frac{w}{2} * dl * \cos\left(\frac{\theta}{2}\right) - \frac{\varepsilon_0(\varepsilon_l - 1){V_0}^2}{2\delta} * dl * \frac{w}{2} \tag{16}$$

therefore, force can be expressed as:

$$\mathrm{F} = \frac{\mathrm{dG}}{\mathrm{dl}} = \gamma_{lg} * \frac{1}{2} * \pi * \frac{w}{2} * \cos\left(\frac{\theta}{2}\right) - \frac{\varepsilon_0(\varepsilon_l - 1){V_0}^2}{2\delta} * \frac{w}{2} \tag{17}$$

Since the liquid is in equilibrium, set total force to zero:

$$\cos\left(\frac{\theta}{2}\right) = \frac{\varepsilon_0(\varepsilon_l - 1)}{\gamma_{lg} * \pi * \delta} * {V_0}^2 \tag{18}$$

Therefore, as voltage increases, top angle of triangle is getting smaller and fluid is elongating. This relationship is examined by experimental data, it is shown below that this ${V_0}^2$ to $\cos\left(\frac{\theta}{2}\right)$ relationship is linear. When voltage is too large, right side equation can be way larger than left and the DEP force overwhelms surface tension and fluid elongates quickly.

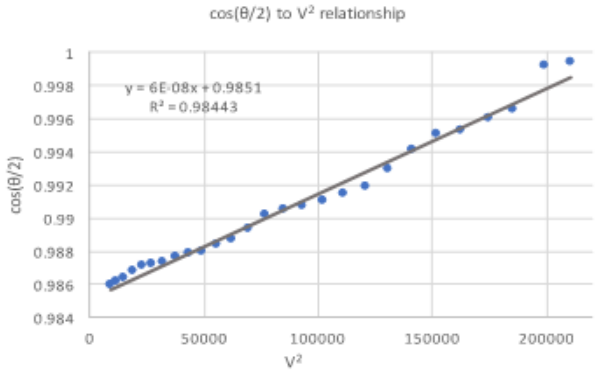

Figure 14. Verification of $\boldsymbol{\cos\left(\frac{\theta}{2}\right)}$ to $\boldsymbol{{V_0}^2}$relationship

As liquid is drawn out at first, the rivulet width is gradually getting bigger. When the width matches the width of electrode, further increase is no longer possible and the surface tension force

reaches a maximum value. As rivulet spreads further, an observation is also noticed that a neck area occurs between the droplet and rivulet. And, as rivulets drives further, this area slowly stretches until it reaches stability. As the neck stretches, rivulet width is gradually increasing, which is also contributing to the increases in surface tension force.

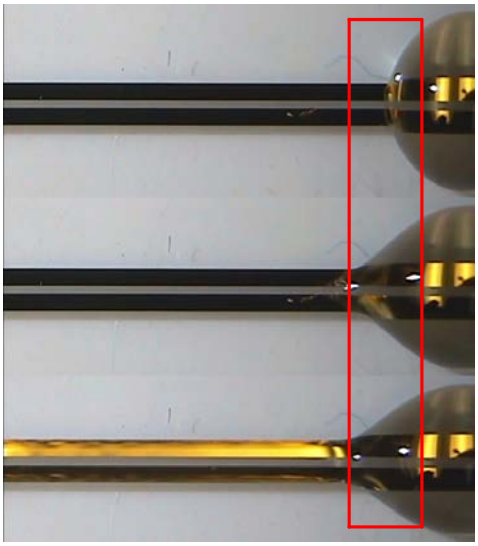

Figure 15. Neck area

In this way, the given phenomenon is reasonably comprehended: as the DEP force grows, a small rivulet is forming and the rivulet width and length increases. When the width finally reaches the maximum value, the neck area stabilizes and the surface tension force reaches its maximum value. As the DEP force continues to grow, it overwhelms the surface tension force and causing the liquid to spread suddenly.

4.0 DRIVING ELECTRODE DESIGNS

4.1 ELECTRODE DESIGNS

Knowing that different shapes have a different threshold voltage, varied shape electrode has been fabricated so as to get different actuation voltage along the electrode. Electrodes with higher actuation voltage on one end and lower on the other was designed and fabricated. To manipulate the actuation voltage on both ends of the electrode, triangular shaped electrodes were introduced. With triangular electrodes shaped like single electrodes in figure 15, varying both electrode width and gap is possible. In this way, controlling via voltage is realized.

Figure 16. Gap/width induced reservoir spreading under increasing voltage

The classic configuration of dielectro-wetting is an electrode panel made up of uniform electrodes [19], which is used as reservoir in this research. By changing the width and gap we can control the area where the fluid is spread. By increasing voltage, fluid spreads to larger area of surface. Also, if width is larger, the electrode can hold more fluid, as seen in the Figure 15. More fluid is accumulated around larger width part.

To test how driving electrode work in the capacitor, the driving electrodes are fabricated with reservoir, and driving feature is tested below.

Figure 17. 200 μm -10 μm width uniform gap electrode induced driving

Uniform gap varying width is fabricated, it is easy to see that this behavior is similar to that of parallel electrodes. At certain voltage, sudden spreading still occurs. Controlling fluid length with voltage is still hard.

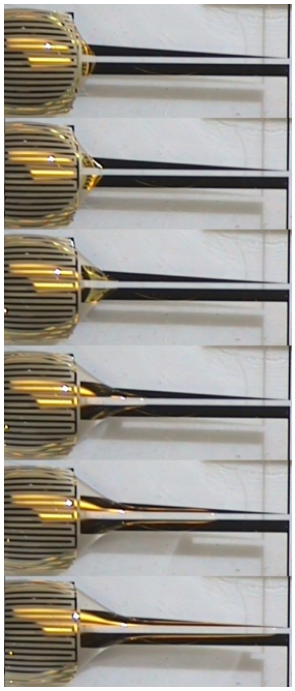

Figure 18. One-sided 200 μm -10 μm Width uniform gap induced driving

Behavior doesn't change much with one side changing width electrode. Length-voltage relationship is similar to that of no width gap changed two parallel square electrodes. Fluid length controlling is still hard to implement.

Below is an electrode with only gap changing:

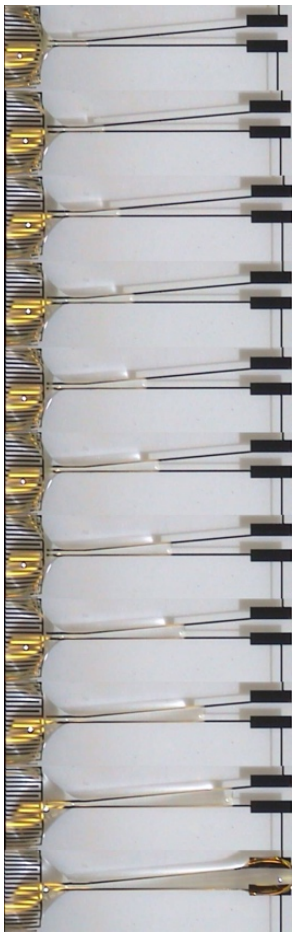

Figure 19. 50 μm width 50-350 μm gap electrode induced driving

In this case, the fluid can change almost linearly. But the problem is that fluid-air interface is not stable, clear small change in voltage can't effectively result in a clear view of fluid length change. Or in other words, there's a time lag controlling the fluid. Also, oscillation is also a main problem during this driving process.

So, electrodes with both width and gap changing are fabricated.

Figure 20. 200 μm width one side triangular electrode other side driving

Another electrode with both width and gap changing was fabricated. It can be seen from length-voltage relationship that this electrode shape can give good controllable relationship of voltage and fluid length. Therefore, different size of this kind of electrode was fabricated with varying electrode width on the reservoir side of electrode. 100, 150, 200 μ m was used as this width, and voltage-length relationship was determined.

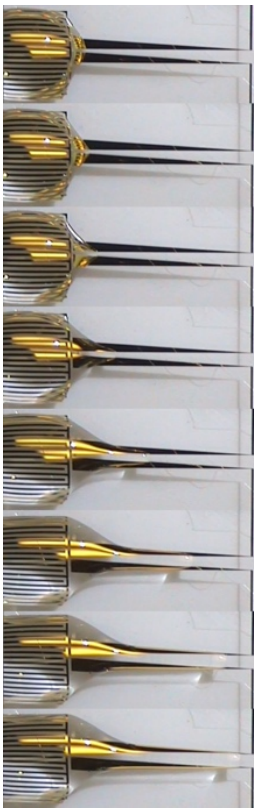

Figure 21. Two 150-10 μm triangular shaped electrode driving

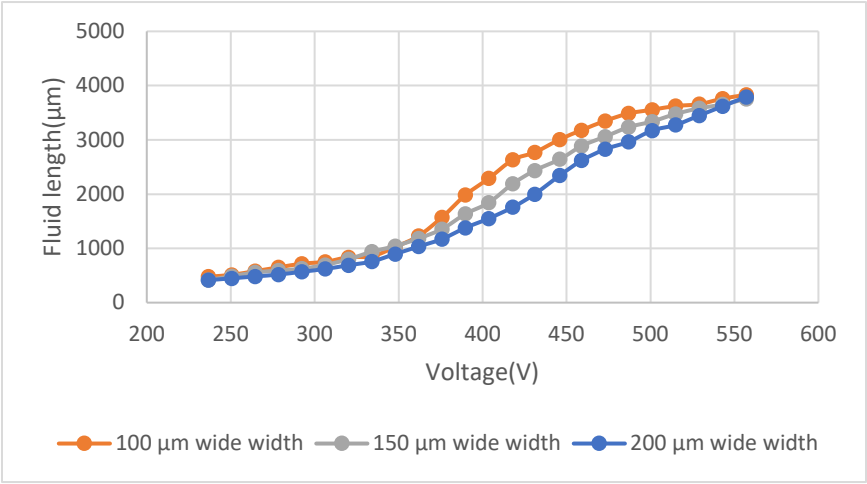

Figure 22. Different size electrode length voltage relationship

With changing gap and width, three similar shape electrodes with different size driving electrodes have been tested, each with the end length increasing. As the slope is increasing, it is obvious to observe that with larger slope, the driving electrode have a better, more linear voltage-length relationship.

In this way, we could say that both width and gap changing is the best way of building a driving electrode, wider electrode width can give a more linear relationship. This kind of electrode is used in the capacitor.

4.2 THEORETICAL ANALYSIS

In this section, theoretical analysis is conducted to explain the observed phenomenon in this chapter. As is shown in chapter 3, the angle in equation 18 can be expressed by length of fluid and width of electrode, in this way, a length voltage relationship is deduced:

$$\frac{l}{\sqrt{l^2 + w^2}} = \frac{\varepsilon_0(\varepsilon_l - 1)}{\gamma_{lg} * \pi * \delta} * {V_0}^2 \tag{19}$$

Penetration depth of electrode can be expressed as:

$$\delta = \frac{4g}{\pi} \tag{20}$$

Where g is the gap between electrode. In this case g is a in linear relationship with length. Therefore, the rough relationship between fluid length and voltage is:

$$\frac{l^2}{\sqrt{l^2 + w^2}} = \frac{\varepsilon_0(\varepsilon_l - 1)}{\gamma_{lg} * \pi} * {V_0}^2$$

At first, when length is relatively small, *w* is relatively big, the denominator of left side equation can be considered as a constant. As length continues to grow, w is relatively getting smaller, and denominator can be considered as a single *l*. The fluid length is then considered to change from first order to second order equation of *l*. So, length voltage relationship can be considered as a transition between first and second order. This can explain the first phase of the slope in Figure 21.

5.0 VOLTAGE CONTROLLED TUNABLE CAPACITOR

5.1 CAPACITANCE ELECTRODE

Two configurations have been chosen as capacitor driving electrode as shown below in the figure. As fluid is driven out of the reservoir gradually, capacitance is measured three times at not covering capacitor, half covering capacitor and fully covering the capacitor. Capacitance is measured to be the largest at when fluid is covering whole capacitor, and smallest at when fluid is not covering capacitor, tuning range is determined using the most covered and least covered condition.

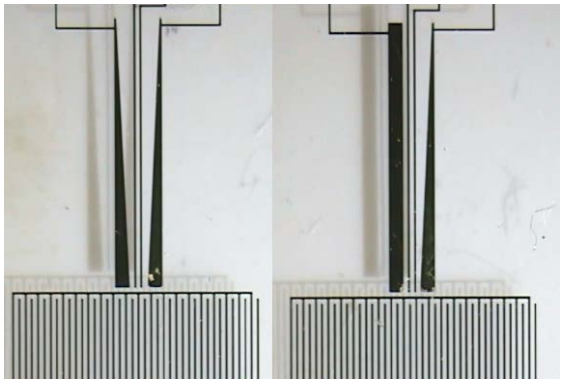

Figure 23. Capacitor patterns

5.2 PERFORMANCE OF CAPACITOR

In order to measure capacitance, the capacitor electrode is connected to a circuit in parallel with a 7.5 μH inductor. Resonance frequency of parallel LC circuit can be expressed as:

$$\mathrm{F} = \frac{1}{2\pi\sqrt{LC}} \tag{19}$$

Therefore, we can get capacitance with the inductance and resonant frequency:

$$\mathrm{C} = \frac{1}{\mathrm{L}} * \frac{1}{(2\pi f)^2} \tag{20}$$

In order to be tested, the electrodes are connected to a square of gold during fabrication, and the square soldered to a piece of electric wire, which is connected to the function generator and amplifier shown in Figure 23.

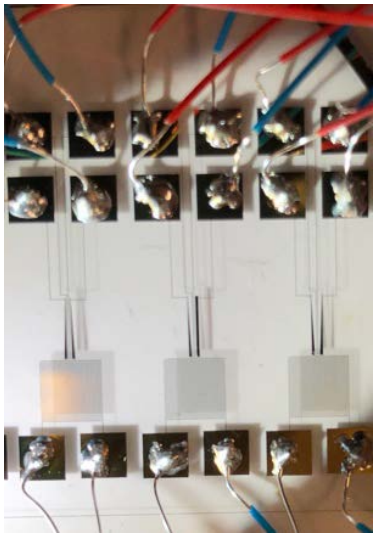

Figure 24. Electrodes and connections

In this case both the squares and the electric wires will become a parasitic capacitance in pico-farad scale. Also, the commercialized inductor has a small amount of parasitic capacitance as well, in this scale, even small capacitance can't be ignored.

In order to reduce this parasitic capacitance influence, a similar circuit is fabricated as reference only without the device part. The capacitance value of this device is measured the same way as the device because either parasitic capacitance from inductor or that from the whole circuit is in parallel with the device capacitance. This capacitance value would be used as parasitic capacitance and deduced from the measured value to get the real capacitance value.

While calculating the capacitance value, a q factor is also read from the impedance analyzer. Figure 24 and Figure 25 are the impedance analyzer data, the peak represents the resonate frequency.

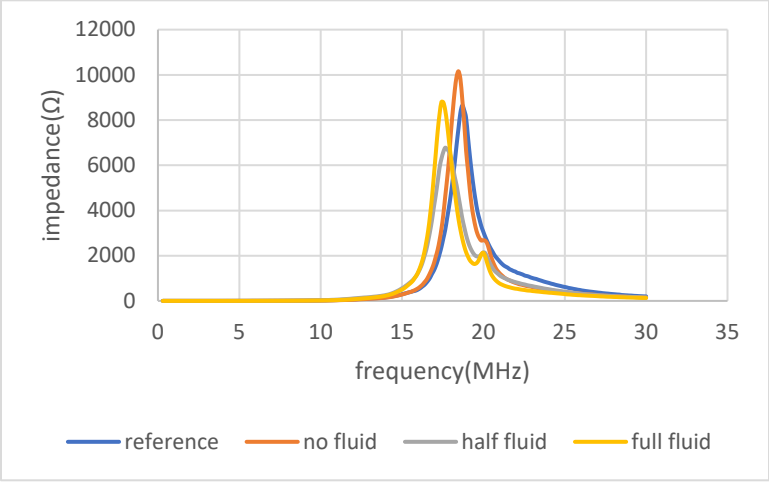

Figure 25. First capacitance measuring

Capacitance tuning range is 0.2-1.4 pF for above figure, capacitance is measured to be 0.9 pF at half fluid.

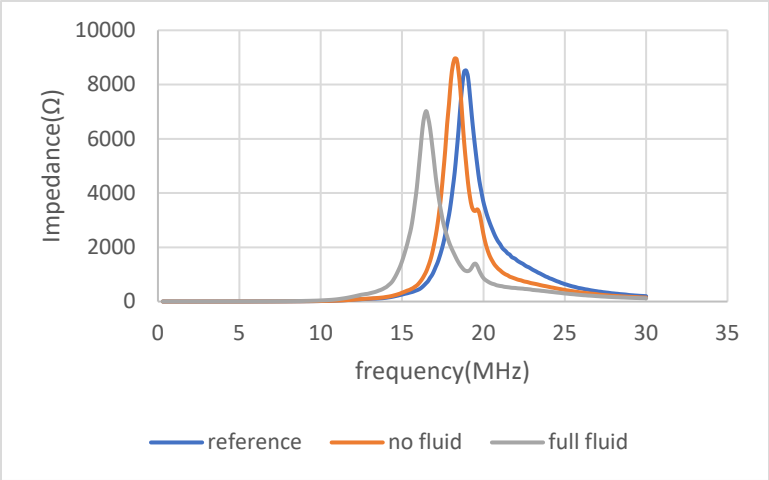

Figure 26. Second capacitor measuring

Capacitance tuning range is 0.7-3.0 pF for above figure. Given the impedance frequency chart, resonance frequency is easy to get. Using equation 20, we can calculate the capacitance of the whole device. Two of the electrodes are tested, and the changing of capacitance is detected. Maximum tuning range is 0.2-1.4pF 0.7-3.0pF, q factor is measured to be 250 and 600 at 3MHz.

Lastly, a voltage-capacitance relationship was drawn out with another device and is shown below:

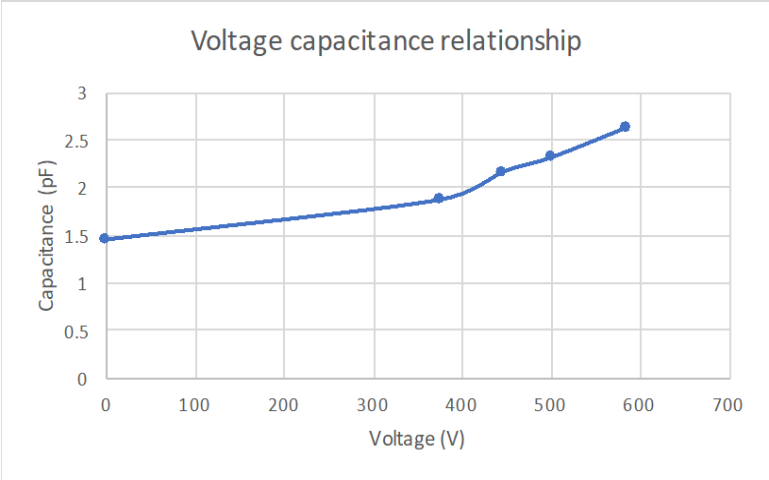

Figure 27. Voltage capacitance relationship

6.0 CONCLUSION AND FUTURE WORK

In this research, two parallel electrode driving electrode were tested under increasing voltage. A simple analysis using Gibbs free energy method was introduced to explain a sudden fierce spreading of fluid along the electrodes. By manipulating the shape of the electrode, dielectric fluid was driven by voltage to move continuously along two electrodes in an almost linear voltage-length relationship. A tunable capacitor is then built by pulling liquid in and out of the capacitor between the electrodes, a 0.7-3.0 pF capacitance was discovered with q factors of 250 at 3MHz.

Since the capacitor electrodes were built in the same plane, electric field between them is mainly a fringing field, which makes its capacitance relatively small. In the future, 3D structure may be utilized to provide a larger capacitance and a clearer tuning range.

BIBLIOGRAPHY

[1] E. Abbaspour-Sani, N. Nasirzadeh, and G. R. Dadashzadeh, "Two Novel Structures for Tunable Mems Capacitor With Rf Applications," *Prog. Electromagn. Res.*, vol. 68, pp. 169–183, 2007.

[2] A. Oz and G. K. Fedder, "RF CMOS-MEMS capacitor having large tuning range," *TRANSDUCERS 2003 - 12th Int. Conf. Solid-State Sensors, Actuators Microsystems, Dig. Tech. Pap.*, vol. 1, no. 412, pp. 851–854, 2003.

[3] F. Khan, Y. Zhu, J. Lu, J. Pal, and D. V. Dao, "A single-layer micromachined tunable capacitor with an electrically floating plate," *Smart Mater. Struct.*, vol. 25, no. 4, 2016.

[4] R. L. Bonvick, P. A. Stupar, J. Denatale, R. Anderson, C. Tsai, and K. Garrett, "A High Q , large tuning range , tunable capacitor for RF applications," *Fifteenth IEEE Int. Conf. Micro Electro Mech. Syst.*, vol. 103, pp. 669–672, 2002.

[5] J. Yoon, C. T. Nguyen, and A. Arbor, "A High- Q Tunable Micromechanical Capacitor With Movable Dielectric for RF Applications," pp. 489–492, 2000.

[6] J. Zou, C. Liu, and J. Schutt-Aine, "Development of a wide tuning range MEMS tunable capacitor for wireless communication systems," … *Devices Meet. 2000* …, vol. 0, no. C, pp. 403–406, 2000.

[7] D. T. Mccormick, Z. Li, and N. Tien, "Capacitors," pp. 3–6, 2003.

[8] S. O. Choi, Y. K. Yoon, M. G. Allen, and A. T. Hunt, "A Tunable Capacitor Using An Immiscible Bifluidic Dielectric," *Comput. Eng.*, no. 1, pp. 873–876, 2004.

[9] H. Habbachi *et al.*, "Study of a tunable MEMS capacitor : influence of fluids To cite this version :," vol. 53, no. 2, pp. 72–73, 2016.

[10] N. Habbachi, H. Boussetta, A. Boukabache, M. A. Kallala, P. Pons, and K. Besbes, "Fabrication and modeling of a capacitor microfluidically tuned by water," *IEEE Electron Device Lett.*, vol. 38, no. 2, pp. 277–280, 2017.

[11] H. A. Pohl, "The motion and precipitation of suspensoids in divergent electric fields," *J. Appl. Phys.*, vol. 22, no. 7, pp. 869–871, 1951.

[12] T. B. Jones, M. Gunji, M. Washizu, and M. J. Feldman, “Dielectrophoretic liquid actuation and nanodroplet formation,” *J. Appl. Phys.*, vol. 89, no. 2, pp. 1441–1448, 2001.

[13] T. B. Jones, “Liquid dielectrophoresis on the microscale,” *J. Electrostat.*, vol. 51–52, no. 1–4, pp. 290–299, 2001.

[14] R. Ahmed, D. Hsu, C. Bailey, and T. B. Jones, “Dispensing picoliter droplets using dielectrophoretic (DEP) microactuation,” *Microscale Thermophys. Eng.*, vol. 8, no. 3, pp. 271–283, 2004.

[15] T. B. Jones, K. L. Wang, and D. J. Yao, “Frequency-dependent electromechanics of aqueous liquids: Electrowetting and dielectrophoresis,” *Langmuir*, vol. 20, no. 7, pp. 2813–2818, 2004.

[16] T. B. Jones, “On the relationship of dielectrophoresis and electrowetting,” *Langmuir*, vol. 18, no. 11, pp. 4437–4443, 2002.

[17] K. Khoshmanesh, S. Nahavandi, S. Baratchi, A. Mitchell, and K. Kalantar-zadeh, “Dielectrophoretic platforms for bio-microfluidic systems,” *Biosens. Bioelectron.*, vol. 26, no. 5, pp. 1800–1814, 2011.

[18] C. Zhang, K. Khoshmanesh, A. Mitchell, and K. Kalantar-Zadeh, “Dielectrophoresis for manipulation of micro/nano particles in microfluidic systems,” *Anal. Bioanal. Chem.*, vol. 396, no. 1, pp. 401–420, 2010.

[19] C. V. Brown, G. G. Wells, M. I. Newton, and G. McHale, “Voltage-programmable liquid optical interface,” *Nat. Photonics*, vol. 3, no. 7, pp. 403–405, 2009.

[20] G. McHale, C. V. Brown, and N. Sampara, “Voltage-induced spreading and superspreading of liquids,” *Nat. Commun.*, vol. 4, pp. 1605–1607, 2013.

[21] G. McHale, C. V. Brown, M. I. Newton, G. G. Wells, and N. Sampara, “Dielectrowetting driven spreading of droplets,” *Phys. Rev. Lett.*, vol. 107, no. 18, pp. 1–4, 2011.

[22] H. Geng, J. Feng, L. M. Stabryla, and S. K. Cho, “Dielectrowetting manipulation for digital microfluidics: creating, transporting, splitting, and merging of droplets,” *Lab Chip*, vol. 17, no. 6, pp. 1060–1068, 2017.

[23] S.-K. Fan, W.-J. Chen, T.-H. Lin, T.-T. Wang, and Y.-C. Lin, “Reconfigurable liquid pumping in electric-field-defined virtual microchannels by dielectrophoresis.,” *Lab Chip*, vol. 9, no. 11, pp. 1590–5, 2009.

[24] S.-K. Fan, Y.-W. Hsu, and C.-H. Chen, 釱涝ncapsulated droplets with metered and removable oil shells by electrowetting and dielectrophoresis," *Lab Chip*, vol. 11, no. 15, p. 2500, 2011.

[25] S.-K. Fan, T.-H. Hsieh, and D.-Y. Lin, "General digital microfluidic platform manipulating dielectric and conductive droplets by dielectrophoresis and electrowetting," *Lab Chip*, vol. 9, no. 9, p. 1236, 2009.

[26] S.-K. Fan and D.-Y. Lin, "Digital Microfluidics with Bubble Manipulations by Dielectrophoresis," *Int. J. Autom. Smart Technol.*, vol. 2, no. 1, pp. 69–74, 2012.

[27] S.-K. Fan, H.-P. Lee, C.-C. Chien, Y.-W. Lu, Y. Chiu, and F.-Y. Lin, "Reconfigurable liquid-core/liquid-cladding optical waveguides with dielectrophoresis-driven virtual microchannels on an electromicrofluidic platform," *Lab Chip*, vol. 16, no. 5, pp. 847–854, 2016.